The Sensitivity of Saturation Transfer Electron Paramagnetic Resonance Spectra to Restricted Amplitude Uniaxial Rotational Diffusion

Eric J. Hustedt and Albert H. Beth
Department of Molecular Physiology & Biophysics, Vanderbilt University School of Medicine, Nashville, Tennessee 37232, USA

ABSTRACT Computational methods have been developed to model the effects of constrained or restricted amplitude uniaxial rotational diffusion (URD) on saturation transfer electron paramagnetic resonance (ST-EPR) signals observed from nitroxide spin labels. These methods, which have been developed to model the global rotational motion of intrinsic membrane proteins that can interact with the cytoskeleton or other peripheral proteins, are an extension of previous work that described computationally efficient algorithms for calculating ST-EPR spectra for unconstrained URD (Hustedt and Beth, 1995, *Biophys. J.* 69:1409–1423). Calculations are presented that demonstrate the dependence of the ST-EPR signal (V'_2) on the width (Δ) of a square-well potential as a function of the microwave frequency, the correlation time for URD, and the orientation of the spin-label with respect to the URD axis. At a correlation time of 10 μs, the V'_2 signal is very sensitive to Δ in the range from 0 to 60°, marginally sensitive from 60° to 90°, and insensitive beyond 90°. Sensitivity to Δ depends on the correlation time for URD with higher sensitivity to large values of Δ at the shorter correlation times, on the microwave frequency, and on the orientation of the spin-label relative to the URD axis. The computational algorithm has been incorporated into a global nonlinear least-squares analysis approach, based upon the Marquardt–Levenberg method (Blackman et al., 2001, *Biophys. J.* 81:3363–3376). This has permitted determination of the correlation time for URD and the width of the square-well potential by automated fitting of experimental ST-EPR data sets obtained from a spin-labeled membrane protein and provided a new automated method for analysis of data obtained from any system that exhibits restricted amplitude URD.

INTRODUCTION

Cell membranes contain a heterogeneous mixture of lipids and proteins in a bilayer configuration where the intrinsic membrane proteins are present at remarkably high local concentrations. In this crowded two-dimensional fluid environment, the intrinsic membrane proteins that traverse the lipid bilayer can interact to form hetero- and homo-oligomeric complexes (Ryan, 1988). Some integral membrane proteins also interact with cytoskeletal proteins or other peripheral membrane proteins to form supramolecular assemblies that can impart unique properties to the membrane or serve as sites for localization of proteins into functional complexes (Luna and Hill, 1992). Unfortunately, in many cases, it has been difficult to elucidate either the oligomeric state of intrinsic membrane proteins or the nature and extent of their interactions with cytoskeletal or peripheral membrane proteins in situ. Consequently, it has also been difficult to accurately determine how the oligomeric state, or other protein–protein interactions, modulates the function of integral membrane proteins.

Classical approaches such as chemical cross-linking (e.g., Staros and Kakkad, 1983), detergent solubilization and estimation of molecular weight of stable assembled complexes (e.g., Casey and Reithmeier, 1991), radiation inactivation and target size analysis (e.g., Cuppoletti et al., 1985), and direct visualization by freeze fracture electron microscopy (e.g., Weinstein et al., 1978) have all contributed to current models of assembly of membrane proteins in the human erythrocyte and in many other cell and subcellular organelle membranes. Despite their general applicability and widespread utilization, each of these methods has limitations that can preclude unambiguous assignment of oligomeric state(s) under native conditions, particularly the dynamic aspects of the interactions. Moreover, these methods do not generally provide direct evidence of the extent or dynamics of interactions with cytoskeletal or peripheral membrane proteins in the intact, fluid membrane.

Various optical and electron paramagnetic resonance (EPR) methods have been developed and used to measure the global rotational dynamics of membrane proteins to gain direct insight into the sizes of the protein complexes and hence the oligomeric state of the protein in situ (Cherry, 1981, 1992; Beth and Robinson, 1989). Due to the anisotropic nature and the high viscosity of the lipid bilayer, the global rotational diffusion of integral membrane proteins has been modeled as uniaxial rotational diffusion (URD) about the membrane normal axis with the rotational diffusion coefficient, $D_{\|}$, being inversely proportional to the cross-sectional area of the integral membrane domain in the plane of the bilayer (Saffman and Delbrück, 1975; Jähnig, 1979). Rotational diffusion rates for integral membrane proteins are on the order of 10^5 s^{-1} or slower. To study dynamics on this time scale, optical spectroscopic techniques that use exogenous molecular probes with long-lived triplet states, such as time-resolved phosphorescence anisotropy decay, time-resolved delayed fluorescence anisotropy decay, or time-resolved absorption anisotropy decay, have

Received for publication 29 May 2001 and in final form 7 September 2001.
Address reprint requests to Albert H. Beth, Department of Molecular Physiology & Biophysics, Vanderbilt University School of Medicine, Nashville, TN 37232-0615. Tel.: 615-322-4235; Fax: 615-322-7236; E-mail: Al.Beth@mcmail.vanderbilt.edu.

0006-3495/01/12/3156/10 $2.00

been developed. Collectively, these methods will be referred to as time-resolved optical anisotropy (TOA) techniques. Various covalent reacting derivatives of eosin and erythrosin, which exhibit appreciable intersystem crossing rates to the triplet state upon photo excitation, have proven to be well suited as exogenous optical probes for measuring the global rotational diffusion of integral membrane proteins (Cherry, 1981, 1992).

An alternative, complementary approach for measuring the very slow global rotational motions of membrane proteins is saturation transfer electron paramagnetic resonance (ST-EPR). ST-EPR, first described by Hyde and Dalton (1972), uses an exogenous, chemically stable nitroxide spin-label to detect the competition between rotational dynamics and spin lattice relaxation (T_{1e}) in the presence of a partially saturating microwave observer field. For a wide range of spin-labeled proteins, the intrinsic T_{1e} is on the order of microseconds, and it has been shown both experimentally (Thomas et al., 1976) and theoretically (Thomas et al., 1976; Robinson and Dalton, 1980; Beth et al., 1983; Hustedt and Beth, 1995) that ST-EPR signals are highly sensitive to rotational correlation times in the microsecond to millisecond time window ($\tau = 1/(6D)$ where D is the rotational diffusion coefficient). Therefore, TOA and ST-EPR are complementary techniques that are sensitive to motions in the same time window.

Both TOA and ST-EPR have the potential to provide direct information on the oligomeric state of proteins in their native membrane, the distribution of different sized species, and the extent of interactions with other proteins via restrictions in the amplitudes of rotational motions (see Wahl, 1975; Robinson and Dalton, 1980; Cherry 1981; Szabo, 1984; Beth and Robinson, 1989). To fully interpret the results of either TOA or ST-EPR studies of the global rotational mobility of integral membrane proteins, it is necessary to consider the effect on the experimental data of the rotational diffusion rate, the orientation of the probe relative to the URD axis, the uniqueness of this orientation, the presence of a restriction on the amplitude of URD, and the presence of a distribution of oligomeric species or multiple species with different degrees of restriction on URD.

Previous work has led to theoretical predictions for the TOA decay of a triplet probe bound to an integral membrane protein undergoing unrestricted URD. Specifically, biexponential decays are predicted with decay times proportional to $1/D_{\|}$ and $1/(4D_{\|})$, where $D_{\|}$ is the rotational diffusion rate (Cherry, 1981). The amplitudes of the two exponential decays and the nonzero value of the residual anisotropy at infinite time, r_{∞}, depend on the orientation of the absorption and emission dipoles to the URD axis. The effect of a restrictive potential on TOA decays has been developed for both a square well and a harmonic well (Wahl, 1975; Szabo, 1984). The results are essentially independent of the shape of the potential for equal root-mean-square angular deviations. The potential has little effect on the exponential decay times in comparison to unrestricted URD, but has a large effect on the amplitudes of the decay terms and r_{∞}. Assuming that the lifetimes of individual oligomeric species are long in comparison with their rates of rotational diffusion, then the results of TOA experiments will be the sum of the contributions from the different-sized species that are present. In general, the amplitude of the decay terms in a TOA experiment will depend on the orientation of the optical probe, the mole fraction of the particular experimental species, and the width of a restrictive potential if one is present. Determining the contributions of these three factors to the amplitudes of the multiexponential anisotropy decay based upon TOA data alone has proven challenging for studies of intrinsic membrane proteins in their native membranes (Blackman et al., 1996). In this work, and in Blackman et al. (2001), it is shown that ST-EPR can provide a means of obtaining additional data that potentially can be used to quantify these factors.

ST-EPR spectra depend in a complex way on the uniaxial rotational diffusion rate and the orientation of the nitroxide A- and g-tensors with respect to the membrane normal axis (see Beth and Robinson, 1989; Hustedt and Beth, 1995). ST-EPR spectroscopy requires the use of nonlinear microwave and Zeeman modulation fields for high sensitivity to the correlation time for rotational motion (Hyde and Dalton, 1972; 1979). The intrinsic T_{1e} (which is analogous to the triplet lifetime in optical experiments), the microwave frequency, and the Zeeman modulation frequency all determine the range of correlation times to which the experiment is sensitive (see Beth and Robinson, 1989). The latter two factors are under experimental control, and the use of multiple microwave and Zeeman modulation frequencies allows multiple "snapshots" of the rotational dynamics to be taken (Beth and Robinson, 1989). To date, the use of ST-EPR to study rotational dynamics of membrane proteins has been hampered by the paucity of computational tools for determining the effects on ST-EPR lineshapes of the rotational diffusion rate, probe orientation, and restrictions on the amplitude of rotational motions.

Empirical parametric methods for qualitatively estimating rotational correlation times from experimental ST-EPR spectra have been reported and used in a wide range of studies (see Thomas et al., 1976; Johnson and Hyde, 1981). However, quantitative analysis requires best-fit simulation of the experimental spectrum to extract rotational dynamics information, particularly in the case of anisotropic rotational diffusion (Robinson and Dalton, 1980; Hustedt et al., 1993; Hustedt and Beth, 1995). Algorithms have been developed for the simulation of ST-EPR spectra for general anisotropic rotational diffusion (Robinson and Dalton, 1980) and for an unconstrained URD model that include the effects of rotational correlation time, probe orientation, microwave frequency and amplitude, and modulation frequency and amplitude (Hustedt and Beth, 1995).

We have now extended the algorithms for simulating the ST-EPR spectra of integral membrane proteins undergoing URD to include the effect of a square-well restriction on the amplitude of rotation. Model calculations define the sensitivity of ST-EPR to the amplitude of URD and how this sensitivity varies as a function of spin-label orientation, microwave frequency, and the correlation time for URD. These algorithms are used in Blackman et al. (2001) to resolve what have been longstanding apparent discrepancies in the results obtained from TOA and ST-EPR experiments on band 3. In particular, trypsin cleavage of the link between the transmembrane and cytoplasmic domains of band 3, which should remove any restriction on URD for that population of band 3 that interacts with the cytoskeleton, has a large effect on TOA decays with no observable change in ST-EPR spectra. Based on the work presented here, a model including the distribution of oligomeric species of band 3 in the membrane and a measure of the flexibility of the cytoplasmic domain of band 3 is developed that is consistent with both TOA and ST-EPR data (Blackman et al., 2001). The algorithm reported in this work is completely general, and, therefore, it should be applicable to analyzing ST-EPR data obtained from any spin-labeled macromolecule undergoing restricted amplitude URD. The current studies extend previous work by Howard et al. (1993) where an algorithm was developed to treat the case of motion in a cone under the assumption of axially symmetric magnetic tensors. Though the use of axially symmetric magnetic tensors precluded the use of this algorithm for direct analysis of experimental data, the calculations of Howard et al. (1993) established sensitivity limits of ST-EPR for detection of restricted amplitude motion for the model considered. The rotation in a cone model used by Howard et al. (1993) is specifically applicable to the study of the wobbling motion of spin-labeled lipids in a bilayer or the rotational motion of spin-labeled myosin head groups. The URD model presented in this work is specifically relevant to the study of large integral membrane proteins. Portions of the current work have been published in an abstract (Hustedt et al., 2000).

METHODS

Analysis of ST-EPR spectra

The method used to calculate the ST-EPR spectra of a nitroxide spin-label undergoing URD in a square-well potential follows directly from the method used previously for unrestricted URD (Hustedt and Beth, 1995). A set of Bloch equations describing the dynamics of the nitroxide spin magnetization in an orientation- and time-dependent magnetic field is used (McCalley et al., 1972; Thomas and McConnell, 1974),

$$\frac{d\vec{M}(\Omega(t), t)}{dt} = \vec{M}(\Omega(t), t) \times \gamma_e\vec{H}(\Omega(t), t) - \Gamma_R[\vec{M}(\Omega(t), t) - M_{eq}] - \Gamma_\Omega\vec{M}(\Omega(t), t), \quad (1)$$

where $\vec{M}(\Omega(t), t)$ is the spin magnetization vector, $\Omega(t)$ is the variable describing the random fluctuations of the nitroxide orientation, Γ_R is a phenomenological operator describing spin relaxation processes, and Γ_Ω is the rotational diffusion operator. The time- and orientation-dependent magnetic field is given by

$$\gamma_e\vec{H}(\Omega(t), t) = [\gamma_e h_1]\hat{i} + [\Delta_\omega(\Omega(t), m_i) + \gamma_e h_m \cos(\omega_m t)]\hat{k}, \quad (2)$$

where γ_e is the gyromagnetic ratio of the electron. h_1 is the microwave field stength, h_m is the Zeeman modulation field amplitude, ω_m is the Zeeman modulation frequency, and

$$\Delta_\omega(\Omega(t), m_i) = \omega_0 - g_{eff}(\Omega(t))\beta_\varepsilon H_0 + m_i A_{eff}(\Omega(t)) \quad (3)$$

is the difference between the microwave frequency, ω_0, and the orientation-dependent resonant frequency of the electron coupled to a nitrogen nucleus in spin state m_i. β_ϵ is the Bohr magneton, H_0 is the applied DC magnetic field, and g_{eff} and A_{eff} are determined from the nitroxide orientation and the principal elements of the g- and A-tensors, respectively, as described in detail previously (Hustedt and Beth, 1995). Pseudosecular terms in the spin Hamiltonian are not rigorously treated in this approach, but are instead incorporated into the A_{eff} term. Although this approximation can lead to errors in calculations at correlation times that are moderate to short on the linear EPR time scale (McCalley et al., 1972), it appears to not have a significant effect on the calculation of ST-EPR spectra at correlation times of 1 μs or longer (Hustedt and Beth, 1995). For unconstrained URD, the rotational diffusion operator is given by

$$\Gamma_\Omega = D_\parallel \frac{\partial^2}{\partial\phi^2}, \quad (4)$$

where $D_\parallel$ is the rotational diffusion coefficient.

Unrestricted URD was previously modeled using a transition rate formalism (Thomas and McConnell, 1974) in which the diffusion is treated as random jumps between adjacent sites on an equally spaced, discrete grid in the angle ϕ,

$$\phi^n = \frac{2\pi(n-1)}{N_\phi - 1} \qquad n = 1, 2, 3, ..., N_\phi, \quad (5)$$

so that

$$\Gamma_\Omega\vec{M}^n \approx \kappa\vec{M}^{n-1} - 2\kappa\vec{M}^n + \kappa\vec{M}^{n+1},$$

where $\kappa = D_\parallel(N_\phi - 1)^2/4\pi^2$ and $\vec{M}^n$, is the magnetization vector corresponding to the orientation ϕ^n.

URD in a square well of width Δ_ϕ is modeled as random jumps between equally spaced sites on an angular grid between $\phi_0 - \Delta_\phi/2$ and $\phi_0 + \Delta_\phi/2$ using reflective boundary conditions,

$$\phi^n = \frac{\Delta_\phi(n-1)}{N_\phi - 1} - \frac{\Delta_\phi}{2} + \phi_0 \qquad n = 1, 2, 3, ..., N_\phi, \quad (6)$$

where

$$\phi_0 = \frac{2\pi(m-1)}{N_{\phi_0} - 1} \quad m = 1, 2, 3, ..., N_{\phi_0}.$$

The center of the square well, ϕ_0, is random; so diffusion is modeled for a number of different values of ϕ_0, and the final simulation is obtained by summing over this additional index (see Eqs. 20 and 21 in Hustedt and Beth, 1995). For a value of Δ_ϕ in degrees,

$$N_\phi = \frac{\Delta_\phi}{6} \tag{8}$$

and

$$N_{\phi_0} = \frac{720}{\Delta_\phi} \tag{9}$$

are approximate minimum values required for convergence

The details concerning the construction and solution of the set of steady-state equations that are obtained from Eq. 1 to yield the V_2' ST-EPR signal are given in Hustedt and Beth (1995). Overmodulation effects have been approximated in the current work. The magnetization is expanded as a Fourier series at harmonics of the Zeeman modulation frequency. The effects of overmodulation, which is routinely used in ST-EPR spectroscopy, are determined by back coupling of the signals at the $(j + 1)$th harmonic of the modulation frequency to those at the jth harmonic. In the previous work of Hustedt and Beth (1995), two different algorithms were developed to treat overmodulation. In algorithm I, the back-coupling terms were treated explicitly and the Fourier series was truncated at the third or fourth harmonic. Using algorithm II, significant reductions in computation time are achieved by neglecting these back-coupling terms and by truncating the calculation at the second harmonic. As has been previously shown by Robinson (1983), Zeeman overmodulation effects can be reliably approximated using effective electron relaxation times, T_{1e}^{eff} and T_{2e}^{eff}, where the effective values are functions of the true relaxation times, the modulation amplitude, and the microwave frequency. Previous analysis of ST-EPR data has shown that this approximation does not significantly alter the τ or probe orientation determined for an unconstrained URD model when compared with calculations that explicitly include Zeeman overmodulation terms (Hustedt and Beth, 1995). All of the calculations in this work were performed for a ^{15}N-nitroxide. The adaptation of the algorithm to calculate line shapes for the naturally abundant ^{14}N-nitroxide is straightforward. Line-shape calculations were carried out on a DEC α21164 600 MHz processor (Microway) running the Windows NT operating system. Each calculation required on the order of 30 min of cpu time. Copies of the algorithm developed in this work that run under Windows NT or under UNIX will be made available upon request.

RESULTS

Figure 1 shows X-, Q-, and W-band V_2' ST-EPR spectra (*solid lines*; *top*, *middle*, *bottom*) that were calculated using an unconstrained URD model at correlation times of 10 μs and 1 ms (*arrows*). These spectra show the dramatic line-shape changes that occur with increasing correlation time, particularly at the higher microwave frequencies. The total integrated signal amplitude (*dashed lines*) also depends on the correlation time with a monotonic increase in magnitude as τ increases throughout the microsecond-to-millisecond time window (Squier and Thomas, 1986). The ST-EPR spectrum of a sample containing two or more different oligomeric species will be the sum of the spectra of the individual components assuming that conversion between the different oligomeric states takes place on a time scale of milliseconds or longer. It is clear from these calculations that larger oligomeric species, with longer correlation times, will contribute disproportionately to the observed spectrum. The variation in the total integrated amplitude with correlation time is itself a function of microwave frequency. As a result, the simultaneous analysis of ST-EPR data collected at multiple microwave frequencies provides an excellent opportunity for identifying and quantifying multiple oligomeric species (Beth and Robinson, 1989).

Overlaid on the simulations for the unconstrained URD model in Fig. 1 are simulations performed for constrained URD at a correlation time of 10 μs and $\Delta = 1°$ or $\Delta = 360°$ (*dotted lines*). As expected, the simulations for $\Delta = 360°$ are nearly identical to the simulations for the unconstrained URD model for the same correlation time, 10 μs, at all three microwave frequencies. The simulations calculated for $\Delta = 1°$ and $\tau = 10$ μs are virtually identical to those calculated for the unconstrained model for $\tau = 1$ ms, demonstrating that the slow-motion limit for ST-EPR spectroscopy can be approached either by having a long correlation time ($\tau \sim 1$ ms) or by having a severely restricted amplitude of motion at a much faster correlation time.

Effects of restricted amplitude URD on ST-EPR spectra

Figure 2 shows calculated V_2' ST-EPR spectra that demonstrate the sensitivity of this signal to the restriction on URD at X-, Q-, and W-band microwave frequencies at one spin-label orientation ($\theta = 30°$, $\phi = 0°$; top, middle, bottom). For the case of a square-well potential and a single diffusing species exhibiting a correlation time of 10 μs, it is apparent that the V_2' signal changes dramatically between $\Delta = 1°$ and 30°, less dramatically between 30° and 60°, and only very subtly between 60° and 90°. The spectra are essentially unchanged for values of Δ between 90 and 360° (data not shown). There is a subtle increase in sensitivity to large values of Δ at the higher microwave frequencies (Q- and W-bands) relative to X-band. However, the increase is rather modest, as demonstrated by comparing the paramaterized X- and Q-band data shown in Figs. 3 and 4. The model calculations shown in Fig. 2 demonstrate that ST-EPR is very sensitive to restricted amplitude URD, with a correlation time of 10 μs, when Δ is in the 0 to 60° range but remarkably insensitive to weaker restrictions.

A critical consideration in establishing the overall sensitivity of ST-EPR to restricted amplitude URD is the orientation of the spin-label with respect to the diffusion axis (see Fig. 2, *upper*, for the definition of reference frame). Spectral sensitivity for selected spin-label orientations relative to the URD axis are defined as a function of Δ in Fig. 3. In constructing Fig. 3, the ratios of spectral amplitudes at defined field positions (see Fig. 2), that have previously been shown to be sensitive to rotational dynamics in the V_2' signal (see Thomas et al., 1976; Johnson and Hyde, 1981; Beth and Robinson, 1989), have been used to illustrate the conclusions drawn from a large number of calculated spec-

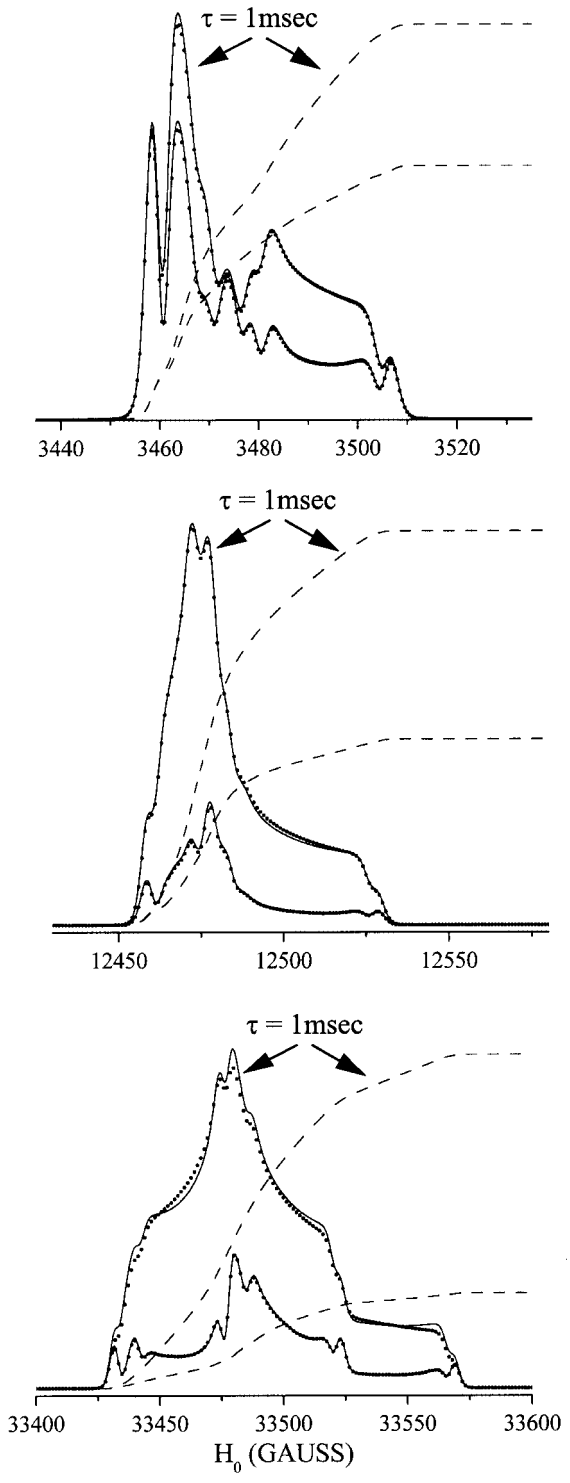

FIGURE 1 Comparison of V_2' ST-EPR spectra of a ^{15}N nitroxide at X-, Q-, and W-band microwave frequencies for unconstrained and constrained URD models. Each panel shows calculated spectra (*solid lines*) for an unconstrained URD model using $\tau = 1$ ms (see *arrows*) and $\tau = 10$ μs together with spectra (*superimposed dotted lines*) calculated for a constrained URD model using $\tau = 10$ μs and $\Delta = 1°$ or $\Delta = 360°$. The dashed lines show the integrated total intensity of the spectra calculated for the unconstrained model. The spectra calculated for $\tau = 1$ ms (unconstrained model) or $\tau = 10$ μs and $\Delta = 1°$ (constrained model, *dotted lines*) exhibit larger total integrated intensity than those calculated for $\tau = 10$ μs (unconstrained model) or $\tau = 10$ μs and $\Delta = 360°$. All spectra were calculated at 50-kHz Zeeman field modulation frequency, $\theta = 30°$, and $\phi = 0°$, $T_{1e}^{eff} = 5$ μs, and $T_{2e}^{eff} = 50$ ns. A microwave observer field of 0.2 Gauss in the rotating frame was used in all calculations.

tra. The ratio parameter data that are plotted in Fig. 3 show that the magnitude of spectral change as a function of the width of the square-well potential depends critically upon the orientation of the spin-label with respect to the URD axis.

To a first approximation, sensitivity of the V_2' signal to rotational motion is proportional to the magnitude of change in the resonance condition that results from the reorientation (i.e., $|\partial H_{res}/\partial\Omega|$ where Ω defines the orientation of the spin-label reference frame with respect to the external magnetic field; Thomas and McConnell, 1974; Beth and Robinson, 1989). The quantity $|\partial H_{res}/\partial\Omega|$ varies in a continuous fashion with field position, from zero when the external magnetic field is parallel to one of the three principal axes of the spin label (principal axis system for the spin label is defined in Fig. 2) to the maximum value at some intermediate orientation that is a function of the A- and g-tensors and the external field strength. From this simplified description, the sensitivity of the V_2' signal to different spin-label orientations can be rationalized.

At X-band, the ratios H''/H and L''/L, and, at Q-band, the ratio E'/E are sensitive to rotational motions about any vector in the *x/y* plane of the spin label (see Fig. 2, *upper*; Beth et al., 1981; Johnson et al., 1982). Hence, high sensitivity to Δ is obtained for $\theta = 90°$ and $\phi = 0°$, where the nitroxide *x* axis is parallel to the diffusion axis, with these ratio parameters as shown in Fig. 3 (*solid squares*). A'/A is sensitive to motions about the spin-label *z* axis. Hence, high sensitivity to Δ is obtained for $\theta = 0°$ and $\phi = 0°$, where the nitroxide *z* axis is parallel to the diffusion axis, with this ratio parameter as shown in Fig. 3, *lower* (*solid diamonds*). Although the magnitude of change of the various ratio parameters depends both on spin-label orientation and on microwave frequency, little change in any of these ratios is seen for values of Δ greater than 60–90° regardless of the orientation or the frequency. These same conclusions apply to parameterized data calculated at W-band (data not shown).

The magnitude of spectral change as a function of Δ also depends upon the correlation time for URD as shown in Fig. 4. For the spin-label orientation model chosen ($\theta = 90°$, $\phi = 0°$; Fig. 2), the largest changes in ratio parameters as a function of Δ (and hence, the largest changes in overall spectral line shapes) are observed at a correlation time of 1 μs (*solid squares*). At this correlation time, measurable changes in the L''/L ratio parameter are observed all the way from 0 to 180°. Reasonably large changes are seen at a correlation time of 10 μs (*solid circles*) out to approxi-

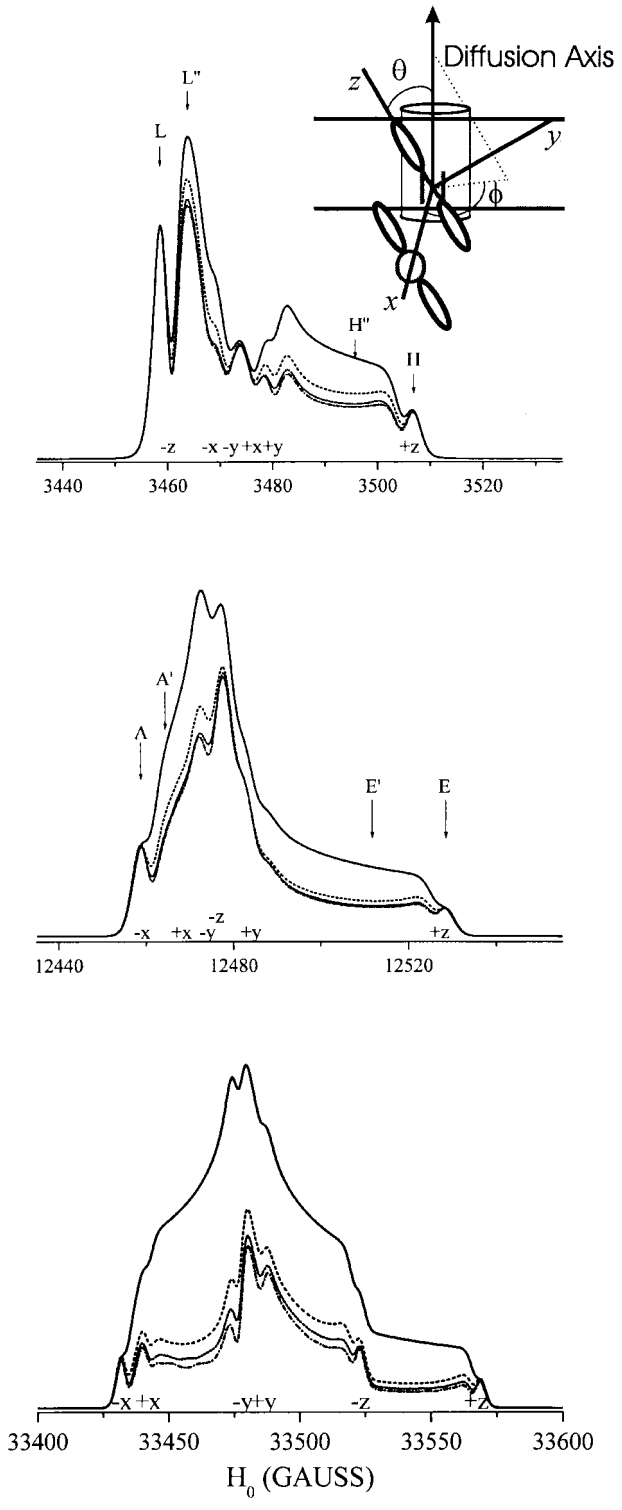

FIGURE 2 Calculated V_2' ST-EPR spectra of a ^{15}N nitroxide at X-band (*top*), Q-band (*middle*), and W-band (*bottom*) for a constrained URD model. Each panel shows spectra calculated for $\Delta = 1°$ (*solid lines*), $\Delta = 30°$ (*dashed lines*), $\Delta = 60°$ (*dotted lines*), and $\Delta = 90°$ (*dot-dash lines*). The spectra were calculated at 50-kHz Zeeman field modulation frequency, $\tau = 10\ \mu s$, $\theta = 30°$, $\phi = 0°$, $T_{1e}^{eff} = 5\ \mu s$, and $T_{2e}^{eff} = 50$ ns. The field positions where spectral amplitudes that are sensitive to Δ are measured are shown superimposed on the calculated spectra at X- and Q-band, whereas the resonance positions for the external field parallel to the *x*-, *y*-, and *z*-axes of the spin label are shown for the $+½$ and $-½$ nuclear manifolds along the field axis. All spectra were normalized so that amplitudes at the $+z$-turning points were approximately equal. The inset defines the angles θ and ϕ that relate the spin-label reference frame to the URD axis.

mately 60°. However, spectral changes are only observed out to values of Δ of 25° at a correlation time of 100 μs (*solid triangles*). When the correlation time is on the order of 1 ms, the V_2' signal is approaching its slow-motion limit, and there is no sensitivity to Δ regardless of spin-label orientation or microwave frequency (data not shown). These calculations show that sensitivity to Δ depends heavily upon the correlation time for URD.

Figure 5 shows a comparison of ratio parameters calculated at X-band for three different URD models. The open circles define the range of variation of L''/L and H''/H as a function of Δ from 0 to 360° for a constrained URD model with $\theta = 90°$, $\phi = 0°$, and $\tau = 1\ \mu s$. The closed squares define the range of L''/L and H''/H as a function of τ for an unconstrained URD model with $\theta = 0°$ and $\phi = 0°$, whereas the closed circles define the range of L''/L and H''/H as a function of τ for an unconstrained URD model with $\theta = 90°$ and $\phi = 0°$. These calculations demonstrate that the ratio parameters, and hence, the spectral line shapes, vary over approximately the same range for vastly different motional models. Therefore, it will not ordinarily be possible to discriminate between motional models nor to extract unique values for the correlation time and the width of a potential by analyzing the line shape from a single measurement. When complex motional models are being evaluated, the importance of combining data obtained at multiple Zeeman field modulation frequencies (Hustedt and Beth, 1995) and multiple microwave frequencies (Blackman et al., 2001) cannot be overemphasized.

DISCUSSION

Saturation transfer EPR was initially developed as an experimental approach to extend the range of sensitivity of conventional EPR into the microsecond-to-millisecond rotational correlation time window (Hyde and Dalton, 1972). A significant motivation behind the development of ST-EPR was the desire to measure the rotational dynamics of large proteins and their assemblies, including integral membrane proteins, to determine the nature and extent of protein–protein interactions. Early work demonstrated the sensitivity of the second-harmonic out-of-phase absorption signal, recorded under conditions of a partially saturating microwave field and with nonlinear Zeeman field modulation, to correlation times throughout this time window (Hyde and Dalton, 1972; Thomas et al., 1976). Early work also showed that the effects of rotational dynamics on the V_2' signal could be accounted for at a qualitative level via

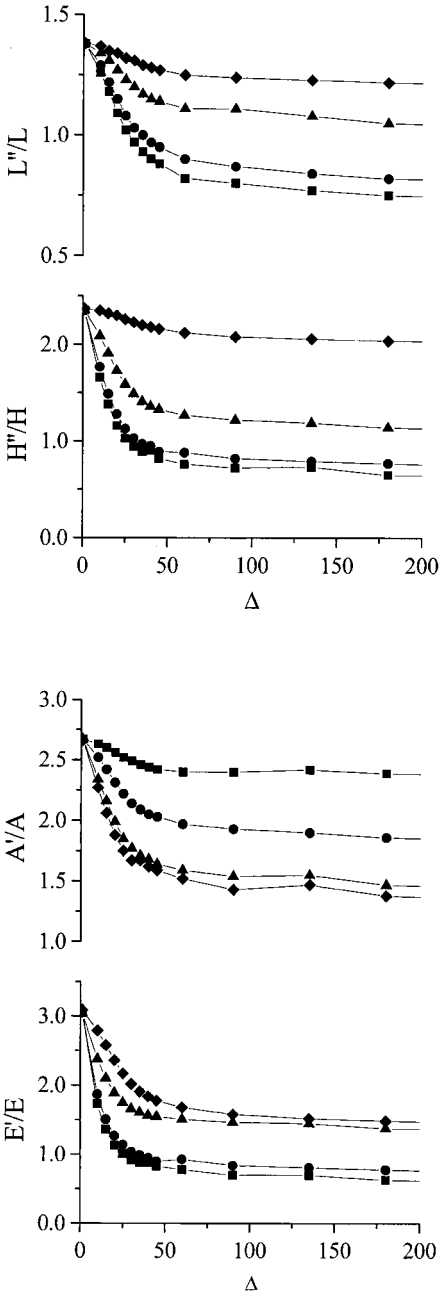

FIGURE 3 Spectral sensitivity plots for V_2' ST-EPR spectra as a function of spin-label orientation relative to the URD axis. The ratios of spectral amplitudes (defined in Fig. 2) are plotted versus Δ for four different spin-label orientations at X-band (9.76 GHz, *upper*) and at Q-band (35.0 GHz, *lower*) microwave frequencies. The angles used were: (♦) $\theta = 0°$, $\phi = 0°$; (▲) $\theta = 30°$, $\phi = 0°$; (●) $\theta = 60°$, $\phi = 0°$; and (■) $\theta = 90°$, $\phi = 0°$. All other parameters were the same as those listed in the legend to Fig. 2.

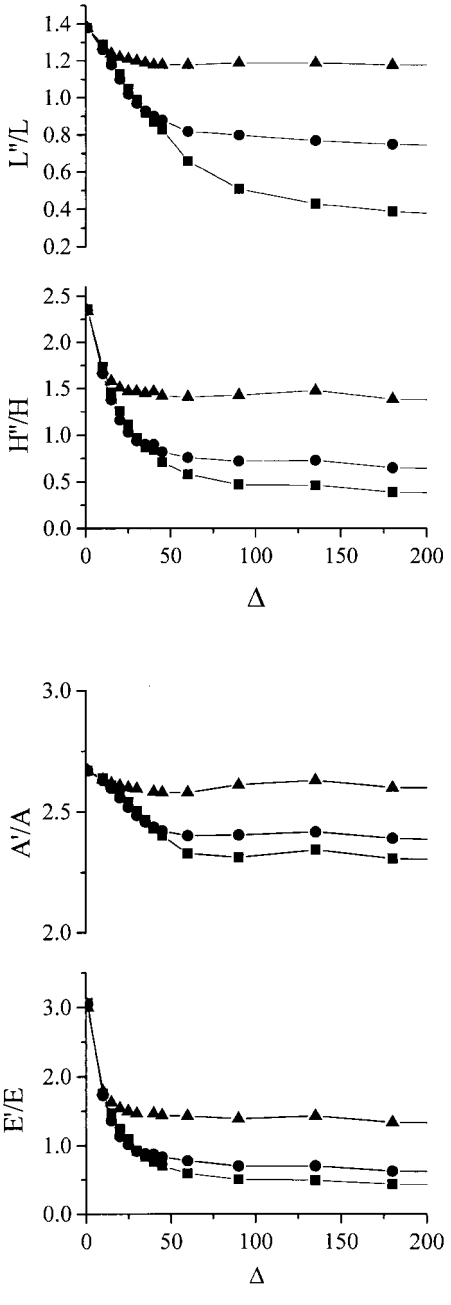

FIGURE 4 Spectral sensitivity plots for V_2' ST-EPR spectra as a function of τ. The ratios of spectral amplitudes are plotted versus Δ for three different rotational correlation times at X-band (9.76 GHz, *upper*) and Q-band (35 GHz, *lower*). The parameters used were: $\theta = 90°$, $\phi = 0°$, $T_{1e}^{eff} = 5\ \mu s$, $T_{2e}^{eff} = 50$ ns, $\upsilon_m = 50$ kHz, and (■) $\tau = 1\ \mu s$, (●) $\tau = 10\ \mu s$, (▲) $\tau = 100\ \mu s$.

development of computational algorithms to calculate signals at correlation times in this regime (Thomas and McConnell, 1974; Thomas et al., 1976). However, given the limited computational speed of computers that were generally available at that time, it was not possible to include sufficient terms in the spin Hamiltonian to permit direct comparison between experiment and theory as a means of extracting dynamics information from experimental data. For example, it was necessary to approximate the A- and g-tensor interactions as axially symmetric and to assume

isotropic rotational diffusion to accelerate the computations. Consequently, at that time, the analysis of ST-EPR data was limited to estimating effective correlation times by comparison of spectral ratio parameters from experimental systems with those obtained from well-defined model systems such as spin-labeled hemoglobin undergoing isotropic rotational diffusion (Thomas et al., 1976; Johnson and Hyde, 1981; see Hyde and Dalton, 1979, and Beth and Robinson, 1989, for extensive discussions of this approach).

Capabilities for extracting correlation times from experimental data were greatly enhanced by the seminal work of Robinson and Dalton (1980) where a computational algorithm that treated the case of unrestricted rigid-body anisotropic motion and that retained full A-, g-, and D-tensor anisotropy was developed. Though computationally demanding at that time, this algorithm was used to characterize the rotational dynamics of spin-labeled proteins including soluble (Beth et al., 1983) and erythroctye membrane-bound glyceraldehyde-3-phosphate dehydrogenase (Beth et al., 1981). With the dramatic increase in computation speed of laboratory-based computers in the past two decades, it became realistic to incorporate computational algorithms into nonlinear least-squares approaches for optimizing the agreement between experimental and calculated data and hence, for testing relevant rotational diffusion models and for extracting rotational correlation times from experimental systems (e.g., Fajer et al., 1990; Hustedt et al., 1993; Wojcicki and Beth, 1993; Budil et al., 1996). However, for this approach to be successful for analyzing V_2' signals, a computationally efficient algorithm was needed that could calculate a complete line shape in a relatively short period of time and that exhibited high numerical stability so that the optimization of the statistics of agreement between experiment and theory could be determined over a wide range of conditions in an automated way.

For the case of unconstrained URD, which is appropriate for the global motion of freely diffusing integral membrane proteins, these criteria were met by the development of an algorithm based upon the transition rate formalism (McCalley et al., 1972; Thomas and McConnell, 1974) as demonstrated in previous work (Hustedt and Beth, 1995). By incorporating this algorithm into a nonlinear least-squares routine based upon the Marquardt–Levenberg approach, the rotational correlation time for spin-labeled band 3 in erythrocyte membrane preparations was determined by optimizing the fit between experimental and calculated spectra (Hustedt and Beth, 1995). Although this work provided evidence that the vast majority of copies of band 3 were undergoing URD about the membrane normal axis (Hustedt and Beth, 1996) of reasonably large amplitude and a rate that was consistent with dimers or tetramers, it remained uncertain whether a constraint to rotational motion might be overlooked in this simple analysis. This concern was based upon the known interactions between the cytoplasmic domain of a subpopulation of band 3 and the membrane skeleton from a wide range of studies (see Low, 1986) and from previous TOA studies that demonstrated a large change in anisotropy decay of the transmembrane domain of band 3 following proteolytic cleavage of the link with the cytoplasmic domain (Nigg and Cherry, 1980).

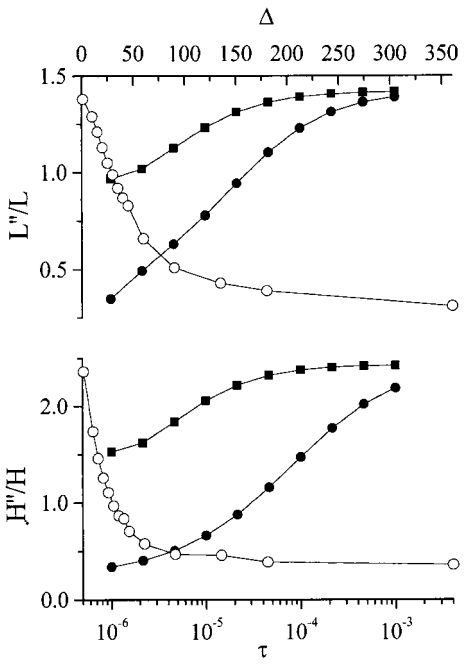

FIGURE 5 Comparison of spectral sensitivity to τ for unconstrained URD and Δ for constrained URD. The ratios of spectral amplitudes at X-band (9.76 GHz) for unconstrained URD are plotted for two different spin-label geometries (■) $\theta = 0°$, $\phi = 0°$; (●) $\theta = 90°$, $\phi = 0°$ as a function of τ on a logarithmic axis (*bottom axis*). The ratios of spectral amplitudes for a constrained URD model ($\theta = 90°$, $\phi = 0°$, $\tau = 1\ \mu s$) are plotted as a function of Δ (*open circles, top axis*). Other parameters used in the calculations include: $T_{1e}^{eff} = 5\ \mu s$; $T_{2e}^{eff} = 50$ ns; and $\upsilon_m = 50$ kHz.

In this work, a computationally efficient algorithm is reported that models the effects of a restrictive square-well potential to URD on ST-EPR spectra as described in Methods. The motivations for this extension of previous work (Hustedt and Beth, 1995) were: 1) to develop a method that could be used to define the sensitivity of ST-EPR signals to a restriction to URD under a wide range of conditions and that could be used to extract the correlation time and amplitude of rotational diffusion from any system that exhibited constrained URD; and 2) to reanalyze the experimental data from spin-labeled band 3 in erythrocyte membranes as described in Blackman et al. (2001). The algorithm that has been developed is perfectly general and it can be used to explore the effects of relevant experimental parameters (e.g., microwave frequency, microwave power, and modulation frequency) and relevant diffusion models (e.g., spin-label orientation, correlation time, and width of the square-well potential) on spectral line shapes. Although it is not feasible to carry out an extensive survey of the effects of all

of these parameters in the current work, the calculations that are described do permit the establishment of some important general conclusions. For example, the data in Fig. 4 show that the absolute sensitivity of the V_2' signal to Δ depends on the correlation time for URD, whereas the data in Fig. 3 provide insights into the effects of spin-label orientation on the sensitivity to Δ. The observation that ST-EPR is most sensitive to small amplitudes of motion is consistent with the work of Howard et al. (1993) using a different model of rotational dynamics. The data in Figs. 1–3 show that the microwave frequency is an important determinant of the magnitude of spectral change that is produced by a restriction to URD. Clearly, this is an experimental variable that can be optimized depending on the correlation time, the spin-label orientation, and Δ in most applications. The data in Fig. 5 demonstrate that Δ can produce the same range of changes in spectral ratio parameters and, hence, V_2' line shapes, as the correlation time for an unrestricted URD model. However, determination of whether an unconstrained or a constrained model best describes the experimental data should be possible by recording V_2' signals under a number of different conditions (e.g., different microwave frequencies and different modulation frequencies) and then comparing the best-fit statistics for these two models following global fitting of the entire data sets (Beth and Robinson, 1989; Hustedt and Beth, 1995).

The calculations in Figs. 2–4 do raise an interesting general point regarding the utilization of ST-EPR to study the global rotational dynamics of macromolecules. Specifically, relatively small amplitude motions can give rise to substantial spectral effects. This means that any local mobility of the spin label or any local dynamic processes that are faster than the global rotational diffusion will give rise to ST-EPR signals that mimic a shorter correlation time. One way to separate local and global contributions to ST-EPR line shapes experimentally is to immobilize the macromolecule under investigation by increasing the viscosity of the solution or by binding it to an appropriate solid support and then recording the ST-EPR signal when global rotational is greatly slowed or entirely prohibited (see Hustedt et al., 1995, for an example of this approach in linear EPR).

The use of multiple microwave frequencies, including microwave frequencies higher than X-band, has become a routine practice in EPR spectroscopy in the past decade, particularly as a means of analyzing complex dynamic processes (e.g., Barnes et al., 1999). ST-EPR studies of rotational dynamics at Q-band have been reported previously (Johnson and Hyde, 1981; Johnson et al., 1982) and as shown in Fig. 3 and in Blackman et al. (2001), this microwave frequency provides higher sensitivity than X-band for observing the effects of constrained URD under some conditions. In particular, Q-band is very sensitive to rotational motions that lead to interconversion of the spin-label *x*- and *y*-axes due to the large field separation provided by the higher magnetic field and the g-tensor anisotropy. Thus, for a constrained URD model where the spin-label *z* axis is aligned with the diffusion axis (Fig. 3, *solid diamonds*), the A'/A parameter measured from the Q-band calculations provides excellent sensitivity to Δ whereas H''/H and L''/L at X-band are very insensitive to Δ. ST-EPR studies of rotational dynamics at W-band have not previously been reported. However, given the increasing availability of EPR spectrometers that operate at W-band, and the capability to calculate V_2' signals at this higher microwave frequency using the algorithm developed in this work, some calculations have been performed to explore the relative sensitivity of the V_2' signal recorded at W-band to Δ as shown in Figs. 1 and 2. The calculations presented in Fig. 2 demonstrate that W-band provides very high sensitivity to small values of Δ (compare the solid lines ($\Delta = 1°$) to the dashed lines ($\Delta = 30°$) at the three microwave frequencies). However, sensitivity to large values of Δ ($\geq 60°$) is not significantly increased relative to the lower microwave frequencies for the URD model shown in Fig. 2 ($\theta = 90°$, $\phi = 0°$). High sensitivity to small values of Δ is also demonstrated by the calculations shown in Fig. 1. Specifically, the W-band calculation for $\Delta = 1°$ is noticeably altered relative to the unconstrained URD calculation at a correlation time of 1 ms whereas the X- and Q-band results for these two situations are virtually indistinguishable. Though an extensive survey of the relative sensitivity of W-band to a wide range of experimental parameters has not been carried out to-date, the results presented here do provide indications that ST-EPR studies at this frequency may be of considerable utility in future investigations. In particular, the simultaneous, global analysis of ST-EPR data collected at X-, Q-, and W-bands should provide a powerful means for discriminating among various diffusion models in a wide range of applications in the future.

The authors wish to thank Drs. Charles Cobb and Hassane Mchaourab (Vanderbilt University) for critiquing the manuscript before submission.

This work was supported by grant R37 HL34737 from the National Institutes of Health.

REFERENCES

Barnes, J. P., Z. Liang, H. S. Mchaourab, J. H. Freed, and W. L. Hubbell. 1999. A multifrequency electron spin resonance study of T4 lysozyme dynamics. *Biophys. J.* 76:3298–3306.

Beth, A. H., K. Balasubramanian, B. H. Robinson, L. R. Dalton, S. D. Venkataramu, and J. H. Park. 1983. Sensitivity of V_2' saturation transfer electron paramagnetic resonance signals to anisotropic rotational diffusion with [^{15}N]nitroxide spin-labels: effects of noncoincident magnetic and diffusion tensor principal axes. *J. Phys. Chem.* 87:359–367.

Beth, A. H., and B. H. Robinson. 1989. Nitrogen-15 and deuterium substituted spin labels for studies of very slow rotational motion. *In* Biological Magnetic Resonance. Vol. VIII, Spin Labeling Theory and Applications. L. J. Berliner and J. Reuben, editors, Plenum Press, New York.179–253.

Beth, A. H., S. D. Venkataramu, K. Balasubramanian, L. R. Dalton, B. H. Robinson, D. E. Pearson, C. R. Park, and J. H. Park. 1981. ^{15}N- and ^{2}H-substituted maleimide spin-labels: improved sensitivity and resolution for biological EPR studies. *Proc. Natl. Acad. Sci. U.S.A.* 78: 967–971.

Blackman, S. M., C. E. Cobb, A. H. Beth, and D. W. Piston. 1996. The orientation of eosin-5-maleimide on human erythrocyte band 3 measured by fluorescence polarization microscopy. *Biophys. J.* 71:194–208.

Blackman, S. M., E. J. Hustedt, C. E. Cobb, and A. H. Beth. 2001. Flexibility of the cytoplasmic domain of the anion exchange protein, band 3, in human erythrocytes. *Biophys. J.* 81:3363-3376.

Budil, D. E., S. Lee, S. Saxena, and J. H. Freed. 1996. Nonlinear-least-squares analysis of slow-motion EPR spectra in one and two dimensions using a modified Levenberg–Marquardt algorithm. *J. Magn. Reson. A.* 120:155–189.

Casey, J. R., and R. A. F. Reithmeier. 1991. Analysis of the oligomeric state of band 3, the anion transport protein of the human erythrocyte membrane, by size exclusion high performance liquid chromatography. *J. Biol. Chem.* 266:15726–15737.

Cherry, R. J. 1981. Rotational diffusion of membrane proteins: measurements with bacteriorhodopsin, band 3 proteins and erythrocyte oligosaccharides. *In* Mobility and Migration of Biological Molecules. P. B. Garland and R. J. P. Williams, editors. The Biochemical Society, London.183–190.

Cherry, R. J. 1992. Rotational diffusion of membrane proteins: studies of band 3 in the human erythrocyte membrane using triplet probes. *In* Structural and Dynamic Properties of Lipids and Membranes. P. J. Quinn and R. J. Cherry, editors. Portland Press, London.137–152.

Cuppoletti, J., J. Goldinger, B. Kang, I. Jo, C. Berenski, and C. Y. Jung. 1985. Anion carrier in the human erythrocyte exists as a dimer. *J. Biol. Chem.* 260:15714–15717.

Fajer, P. G., R. H. Bennett, C. F. Polnaszek, E. A. Fajer, and D. D. Thomas. 1990. General method for multiparameter fitting of high-resolution EPR spectra using a simplex algorithm. *J. Magn. Reson.* 88:111–125.

Howard, E. C., K. M. Lindhal, C. F. Polnaszek, and D. D. Thomas. 1993. Simulation of saturation transfer electron paramagnetic resonance spectra for motion with restricted angular amplitude. *Biophys. J.* 64:581–593.

Hustedt, E. J., and A. H. Beth. 1995. Analysis of saturation transfer electron paramagnetic resonance spectra of a spin-labeled integral membrane protein, band 3, in terms of the uniaxial rotational diffusion model. *Biophys. J.* 69:1409–1423.

Hustedt, E. J., and A. H. Beth. 1996. Determination of the orientation of a band 3 affinity spin-label relative to the membrane normal axis of the human erythrocyte. *Biochemistry.* 35:6944–6954.

Hustedt, E. J., S. M. Blackman, C. E. Cobb, and A. H. Beth. 2000. Effects of constrained uniaxial rotational diffusion on ST-EPR spectra: application to band 3 in the human erythrocyte. *Biophys. J.* 78:382A.

Hustedt, E. J., C. E. Cobb, A. H. Beth, and J. M. Beechem. 1993. Measurement of rotational dynamics by the simultaneous non-linear analysis of optical and EPR data. *Biophys. J.* 64:614–621.

Hustedt, E. J., J. J. Kirchner, A. Spaltenstein, P. B. Hopkins, and B. H. Robinson. 1995. Monitoring DNA dynamics using spin-labels with different independent mobilities. *Biochemistry.* 34:4369–4375.

Hyde, J. S., and L. R. Dalton. 1972. Very slow tumbling spin labels: adiabatic rapid passage. *Chem. Phys. Lett.* 16:568–572.

Hyde, J. S., and L. R. Dalton. 1979. Saturation transfer spectroscopy. *In* Spin Labeling II: Theory and Applications. L. J. Berliner, editor. Academic Press, New York. 1–70.

Jähnig, F. 1979. The shape of a membrane protein derived from rotational diffusion. *Eur. Biophys. J.* 14:63–64.

Johnson, M. E., and J. S. Hyde. 1981. 35-GHz (Q-band) saturation transfer electron paramagnetic resonance studies of rotational diffusion. *Biochemistry.* 20:2875–2880.

Johnson, M. E., L. Lee, and L. W.-M. Fung. 1982. Models for slow anisotropic rotational diffusion in saturation transfer electron paramagnetic resonance at 9 and 35 GHz. *Biochemistry.* 21:4459–4467.

Low, P. S. 1986. Structure and function of the cytoplasmic domain of band 3: center of erythrocyte membrane-peripheral protein interactions. *Biochim. Biophys. Acta.* 864:145–167.

Luna, E. J., and A. L. Hill. 1992. Cytoskeleton—plasma membrane interactions. *Science.* 258:955–964.

McCalley, R. C., E. J. Shimshick, and H. M. McConnell. 1972. The effect of slow rotational motion on paramagnetic resonance spectra. *Chem. Phys. Lett.* 13:115–119.

Nigg, E. A., and R. J. Cherry. 1980. Anchorage of a band 3 population at the erythrocyte cytoplasmic membrane surface: protein rotational diffusion measurements. *Proc. Natl. Acad. Sci. U.S.A.* 77:4702–4706.

Robinson, B. H. 1983. Effects of overmodulation on saturation transfer EPR signals. *J. Chem. Phys.* 72:1312–1324.

Robinson, B. H., and L. R. Dalton. 1980. Anisotropic rotational diffusion studied by passage saturation transfer electron paramagnetic resonance. *J. Chem. Phys.* 72:1312–1324.

Ryan, T. A., J. Myers, D. Holowka, B. Baird, and W. W. Webb. 1988. Molecular crowding on the cell surface. *Science.* 239:61–64.

Saffman, P. G., and M. Delbrück. 1975. Brownian motion in biological membranes. *Proc. Natl. Acad. Sci. U.S.A.* 72:3111–3113.

Squier, T. C., and D. D. Thomas. 1986. Methodology for increased precision in saturation transfer electron paramagnetic resonance studies of rotational dynamics. *Biophys. J.* 49:921–935.

Staros, J. V., and B. P. Kakkad. 1983. Cross-linking and chymotryptic digestion of the extracytoplasmic domain of the anion exchange channel in intact human erythrocytes. *J. Membr. Biol.* 74:247–254.

Szabo, A. 1984. Theory of fluorescence depolarization in macromolecules and membranes. *J. Chem. Phys.* 81:150–167.

Thomas, D. D., L. R. Dalton, and J. S. Hyde. 1976. Rotational diffusion studied by passage saturation transfer electron paramagnetic resonance. *J. Chem. Phys.* 65:3006–3024.

Thomas, D. D., and H. M. McConnell. 1974. Calculation of paramagnetic resonance spectra sensitive to very slow rotational motion. *Chem. Phys. Lett.* 25:470–475.

Wahl, P. 1975. Fluorescence anisotropy of chromophores rotating between two reflecting barriers. *Chem. Phys.* 7:210–219.

Weinstein, R. S., J. K. Khodadad, and T. L. Steck. 1978. Fine structure of the band 3 protein in human red cell membranes: freeze-fracture studies. *J. Supramolec. Struct.* 8:325–335.

Wojcicki, W. E., and A. H. Beth. 1993. Structural and binding properties of the stilbenedisulfonate sites on erythrocyte band 3: and electron paramagnetic resonance study using spin-labeled stilbenedisulfonates. *Biochemistry.* 32:9454–9464.